

Bottomonium suppression in nucleus-nucleus collisions using effective fugacity quasi-particle model

Indrani Nilima ^{a*} and Vineet Kumar Agotiya^{a†}

^aCentre for Applied Physics, Central University of Jharkhand Ranchi, India, 835 205

In the present article, we have studied the equation of state and dissociation temperature of bottomonium state by correcting the full Cornell potential in isotropic medium by employing the effective fugacity quasi-particle Debye mass. We had also calculated the bottomonium suppression in an expanding, dissipative strongly interacting QGP medium produced in relativistic heavy-ion collisions. Finally we compared our results with experimental data from RHIC 200GeV/nucleon Au-Au collisions, LHC 2.76 TeV/nucleon Pb-Pb, and LHC 5.02 TeV/nucleon Pb-Pb collisions as a function of number of participants.

KEYWORDS: Equation of State, Strongly Coupled Plasma, Heavy Quark Potential, String Tension, Dissociation Temperature, Quasi-particle Debye mass

PACS numbers: 25.75.-q; 24.85.+p; 12.38.Mh ; 12.38.Gc, 05.70.Ce, 25.75.+r, 52.25.Kn

I. INTRODUCTION

At the Relativistic Heavy-Ion Collider (RHIC) situated at Brookhaven National Laboratory (BNL) heavy-ion collisions have been studied. After the pioneer work done in the direction of suppression by Matsui and Satz, and some other development of the potential models, suppression was observed by both SPS and RHIC [1]. Due to the Debye screening of the Quantum Chromo-Dynamic (QCD) potential between the two heavy quarks, quarkonia suppression was originally claimed to be an unambiguous signal of the formation of a Quark-Gluon Plasma (QGP). Quarkonia suppression was suggested to be a signature of the QGP and we can measure the suppression (Υ as well as J/ψ), both at RHIC and at the LHC.

In heavy-ion collisions to determine the properties of the medium formed in A+A collisions and p + p collisions and whether the A+A collision deviates from simple superposition of independent p + p collisions. This deviation is quantified with the nuclear modification factor (R_{AA}). This factor is the ratio of the yield in heavy-ion collisions over the yield in p + p collisions, scaled by a model of the nuclear geometry of the collision. The value of $R_{AA}=1$ indicates no modification due to the medium. We can say that the probe of interest is suppressed in heavy-ion collisions if R_{AA} is less than 1. A quarkonia meson that forms on the outside surface will not dissociate regardless of the temperature of the medium because

it doesn't have a chance to interact with it. This is why we never see a R_{AA} that is equal to zero. The suppression can also be affected by the QGP, the formation time of the quarkonia meson and the QGP lifetime as well. For instance, a high p_T quarkonia meson could have a formation time long enough that it actually does not see the QGP at all and thus isn't suppressed.

In the early days most of the interests were focused on the suppression of charmonium states [1, 2] of collider experiments at SPS and RHIC, but several observations are yet to be understood *namely* the suppression of ψ (1S) does not increase from SPS to RHIC, even though the centre-of-mass energy is increased by fifteen times. The heavy-ion program at the LHC may resolve those puzzles because the beam energy and luminosity are increased by ten times of that of the RHIC. Moreover the CMS detector has excellent capabilities for muon detection and provides measurements of ψ (2S) and the Υ family, which enables the quantitative analysis of quarkonia. That is why the interest may be shifted to the bottomonium states at the LHC energy.

A potential model for the phenomenological descriptions of heavy quarkonium suppression would be quite useful in spite of the progress of direct lattice QCD based determinations of the potential. The large mass of heavy quarks and its small relative velocity, makes the use of non-relativistic quantum mechanics justifiable to describe the quarkonia in the potential models. This is one of the main goals of this present study and argue for the modification of the full Cornell potential as an appropriate potential for heavy quarkonium at finite temperature. QGP created at RHIC have a very low viscosity to entropy ratio i.e. $\eta/S \geq 1/4\pi$ [3–6] and in the non-perturbative domain of QCD, temperature close to T_c the quark matter in the QGP phase is strongly interacting.

In the present paper, we shall employ quasi-particle model for hot QCD equations of state [7, 8] to extract the Debye mass [9] which is obtained in terms of quasi-particle degrees of freedom. We first obtained the medium modified heavy quark potential in isotropic medium and estimate the dissociation temperature. Here, we have used the viscous hydrodynamics to define the dynamics of the system

*Electronic address: nilima.ism@gmail.com

†Electronic address: agotiya81@gmail.com

created in the heavy ion collisions. We have included only the shear viscosity and not included the bulk viscosity. We will look the issue of bulk viscosity in near future.

Our work is organized as follows. In Sec.II., we briefly discuss our recent work on medium modified potential in isotropic medium. In the subsections II (a) and (b) we study the real and imaginary part of the potential in the isotropic medium and Effective fugacity quasi-particle model(EQPM) in subsection (c). In section III we studied about binding energy and dissociation temperature of Υ , Υ' and χ_b state considering isotropic medium. Using this effective potential and by incorporating quasi-particle debye mass, we have then developed the equation of state for strongly interacting matter and have shown our results on pressure, energy density and speed of sound etc. along with the lattice data. In Sec.IV, we have employed the aforesaid equation of state to study the suppression of bottomonium in the presence of viscous forces and estimate the survival probability in a longitudinally expanding QGP. Results and discussion will be presented in Sec.V and finally, we conclude in Sec.VI.

II. MEDIUM MODIFIED EFFECTIVE POTENTIAL IN ISOTROPIC MEDIUM

We can obtain the medium-modification to the vacuum potential by correcting its both Coulombic and string part with a dielectric function $\epsilon(p)$ encoding the effect of deconfinement [10]

$$V(r, T) = \int \frac{d^3\mathbf{p}}{(2\pi)^{3/2}} (e^{i\mathbf{p}\cdot\mathbf{r}} - 1) \frac{V(p)}{\epsilon(p)}, \quad (1)$$

Here the functions, $\epsilon(p)$ and $V(p)$ are the Fourier transform (FT) of the dielectric permittivity and Cornell potential respectively. After assuming r -as distribution ($r \rightarrow r \exp(-\gamma r)$) we evaluated the Fourier transform of the linear part $\sigma r \exp(-\gamma r)$ as

$$-\frac{i}{p\sqrt{2\pi}} \left(\frac{2}{(\gamma - ip)^3} - \frac{2}{(\gamma + ip)^3} \right). \quad (2)$$

While putting $\gamma = 0$, we can write the FT of the linear term σr as,

$$(\tilde{\sigma r}) = -\frac{4\sigma}{p^4\sqrt{2\pi}}. \quad (3)$$

Thus the FT of the full Cornell potential becomes

$$V(p) = -\sqrt{(2/\pi)} \frac{\alpha}{p^2} - \frac{4\sigma}{\sqrt{2\pi}p^4}. \quad (4)$$

To obtain the real and imaginary parts of the potential, we put the temporal component of real and

imaginary part in terms of retarded (or advanced) and symmetric parts in the Fourier space in isotropic medium which finally gives,

$$\begin{aligned} \text{Re}D_{11}^{00}(\omega, p) &= \frac{1}{2} (D_R^{00} + D_A^{00}) \\ \text{and } \text{Im}D_{11}^{00}(\omega, p) &= \frac{1}{2} D_F^{00}. \end{aligned} \quad (5)$$

Let us now discuss, the real and imaginary part of the potential modified using the above define $\text{Re}D_{11}^{00}(\omega, p)$ and $\text{Im}D_{11}^{00}(\omega, p)$ along with Effective fugacity quasi-particle model (EQPM) in the next sub-sections.

A. Real part of the potential in the isotropic medium

Now using the real part of retarded (advanced) propagator in isotropic medium we get

$$\text{Re}D_{R,A}^{00}(0, p) = -\frac{1}{(p^2 + m_D^2)}, \quad (6)$$

whereas the real-part of the dielectric permittivity (also given in [14–16]) becomes

$$\epsilon(p) = \left(1 + \frac{m_D^2}{p^2} \right). \quad (7)$$

Now using Eq.6 and real part of dielectric permittivity Eq.7 in Eq.1 we get,

$$\begin{aligned} \text{Re}V_{(iso)}(r, T) &= \int \frac{d^3\mathbf{p}}{(2\pi)^{3/2}} (e^{i\mathbf{p}\cdot\mathbf{r}} - 1) \left(-\sqrt{(2/\pi)} \frac{\alpha}{p^2} - \frac{4\sigma}{\sqrt{2\pi}p^4} \right) \\ &\quad \times \left(\frac{p^2}{(p^2 + m_D^2)} \right) \end{aligned} \quad (8)$$

Solving the above integral, we find

$$\begin{aligned} \text{Re}V_{(iso)}(\hat{s}, T) &= \left(\frac{2\sigma}{m_D} - \alpha m_D \right) \frac{e^{-\hat{s}}}{\hat{s}} - \frac{2\sigma}{\hat{s}} \\ &\quad + \frac{2\sigma}{m_D} - \alpha m_D, \end{aligned} \quad (9)$$

where $\hat{s} = rm_D$. In the limit $\hat{s} \ll 1$, we have

$$\text{Re}V_{(iso)}(\hat{s}, T) \approx -\frac{2\sigma}{m_D\hat{s}} - \alpha m_D, \quad (10)$$

B. Imaginary part of the potential in the isotropic medium

To obtain the imaginary part of the potential in the QGP medium, the temporal component of the

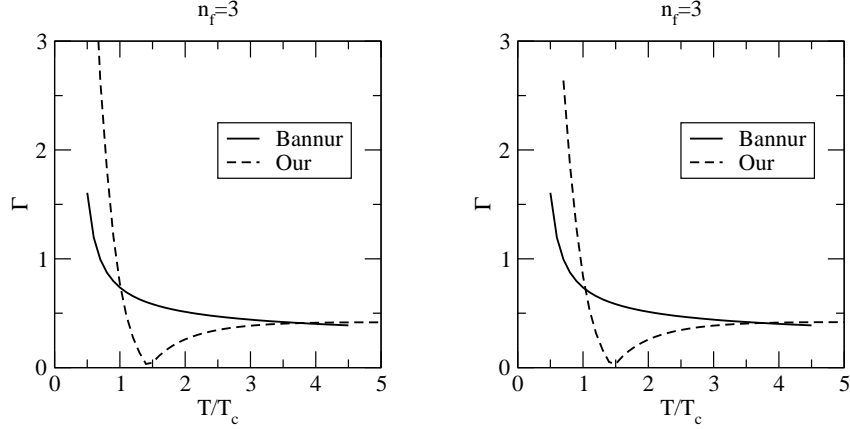


FIG. 1: Plots of Γ as a function of T/T_c for 3flavor QGP (extreme left figure) for EOS1 [11, 12] and for EOS2 [13] (extreme right figure). In each figure, solid line represents the results obtained from Bannur EoS, dashed line represents the results from our EoS (using quasi-particle Debye mass).

symmetric propagator from in the static limit has been considered, which reads [19, 20],

$$ImD_{F(iso)}^{00}(0, k) = \frac{-2\pi T m_D^2}{k(k^2 + m_D^2)^2}. \quad (11)$$

Now the imaginary part of the dielectric function in the QGP medium as:

$$\frac{1}{\epsilon(k)} = -\pi T m_D^2 \frac{k^2}{k(k^2 + m_D^2)^2}. \quad (12)$$

Afterwards, the imaginary part of the in medium potential is easy to obtain owing the definition of the potential Eq. (1) as done in [21]:

$$ImV(r, T) = - \int \frac{d^3 \mathbf{k}}{(2\pi)^{3/2}} (e^{i\mathbf{k} \cdot \mathbf{r}} - 1) \times \left(-\sqrt{\frac{2}{\pi}} \frac{\alpha}{k^2} - \frac{4\sigma}{\sqrt{2\pi k^4}} \right) \frac{-\pi T m_D^2 k}{(k^2 + m_D^2)^2} \quad (13)$$

After performing the integration, we find

$$ImV_{(iso)}(\hat{s}, T) = T \left(\frac{\alpha \hat{s}^2}{3} - \frac{\sigma \hat{s}^4}{30 m_D^2} \right) \log\left(\frac{1}{\hat{s}}\right). \quad (14)$$

where $(\hat{s}) = r m_D$

C. Effective fugacity quasi-particle model(EQPM)

In our calculation, we use the Debye mass m_D for full QCD:

$$m_D^2 = g^2(T) T^2 \left[\left(\frac{N_c}{3} \times \frac{6 PolyLog[2, z_g]}{\pi^2} \right) + \left(\frac{N_f}{6} \times \frac{-12 PolyLog[2, -z_q]}{\pi^2} \right) \right]. \quad (15)$$

Here, $g(T)$ is the QCD running coupling constant, $N_c = 3$ ($SU(3)$) and N_f is the number of flavor, the function $PolyLog[2, z]$ having form, $PolyLog[2, z] = \sum_{k=1}^{\infty} \frac{z^k}{k^2}$ and z_g is the quasi-gluon effective fugacity and z_q is quasi-quark effective fugacity. These distribution functions are isotropic in nature. These fugacities should not be confused with any conservations law (number conservation) and have merely been introduced to encode all the interaction effects at high temperature QCD. Both z_g and z_q have a very complicated temperature dependence and asymptotically reach to the ideal value unity [8]. The temperature dependence z_g and z_q fits well

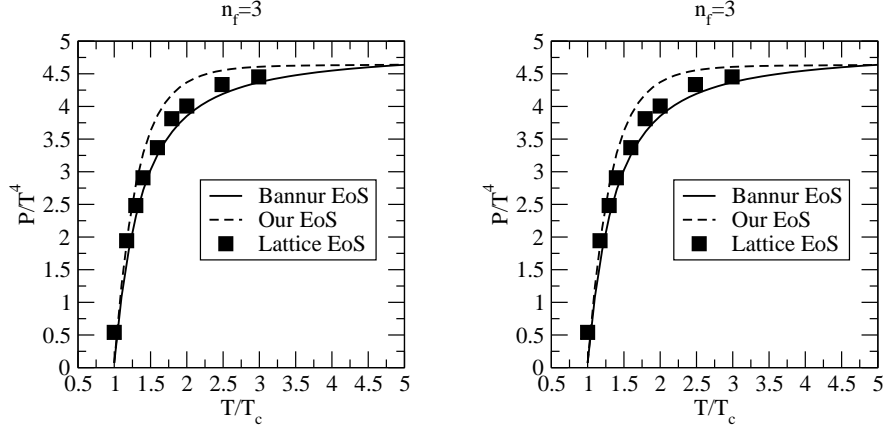


FIG. 2: Plots of P/T^4 as a function of T/T_c for 3-flavor QGP (extreme left figure) for EOS1 [11, 12] and for EOS2 [13] (extreme right figure). In each figure, solid line represents the results obtained from Bannur EoS, dashed line represents the results from Our EoS and diamond symbols represent lattice results [17, 18].

to the form given below,

$$z_{g,q} = a_{g,q} \exp \left(-\frac{b_{g,q}}{x^2} - \frac{c_{g,q}}{x^4} - \frac{d_{g,q}}{x^6} \right). \quad (16)$$

(Here $x = T/T_c$ and a, b, c and d are fitting parameters), for both EOS1 and EOS2. Here, EoS1 is the $O(g^5)$ hot QCD [11, 12] and EoS2 is the $O(g^6 \ln(1/g))$ hot QCD EoS [13] in the quasi-particle description [7, 8] respectively. Now, the expressions for the Debye mass can be rewritten in terms of effective charges for the quasi-gluons and quarks as:

$$m_D^2 = \begin{cases} Q_g^2 T^2 \frac{N_c}{3} & \text{for pure gauge,} \\ T^2 \left(\frac{N_c}{3} Q_g^2 \right) + \left(\frac{N_f}{6} Q_q^2 \right) & \text{for full QCD} \end{cases} \quad (17)$$

where, Q_g and Q_q are the effective charges given by the equations:

$$\begin{aligned} Q_g^2 &= g^2(T) \frac{6 \text{PolyLog}[2, z_g]}{\pi^2} \\ Q_q^2 &= g^2(T) \frac{-12 \text{PolyLog}[2, -z_q]}{\pi^2}. \end{aligned} \quad (18)$$

In our present analysis we had used the temperature dependence of the quasi-particle Debye mass, m_D^{QP} in full QCD with $N_f = 3$ to determine charmonium suppression in an expanding, dissipative

strongly interacting QGP medium. This quasi-particle Debye mass, m_D^{QP} has the following form:

$$m_D^{QP} = \frac{2}{\pi^2} g(T) T \left[\frac{N_c}{3} \text{PolyLog}[2, z_g] - N_f \text{PolyLog}[2, -z_q] \right]^{\frac{1}{2}}. \quad (19)$$

III. BINDING ENERGY AND DISSOCIATION TEMPERATURE

To obtain the binding energies with heavy quark potential we need to solve the Schrödinger equation numerically. In the limiting case discussed earlier, the medium modified potential resembles to the hydrogen atom problem [1]. The solution of the Schrödinger equation gives the eigenvalues for the ground states and the first excited states in charmonium (J/ψ , ψ' etc.) and bottomonium (Υ , Υ' etc.) spectra :

$$\text{Re } E_{\text{bin}}^{\text{iso}} \stackrel{s \gg 1}{\approx} \left(\frac{m_Q \sigma^2}{m_D^4 n^2} + \alpha m_D \right); \quad n = 1, 2, \dots \quad (20)$$

where m_Q is the mass of the heavy quark.

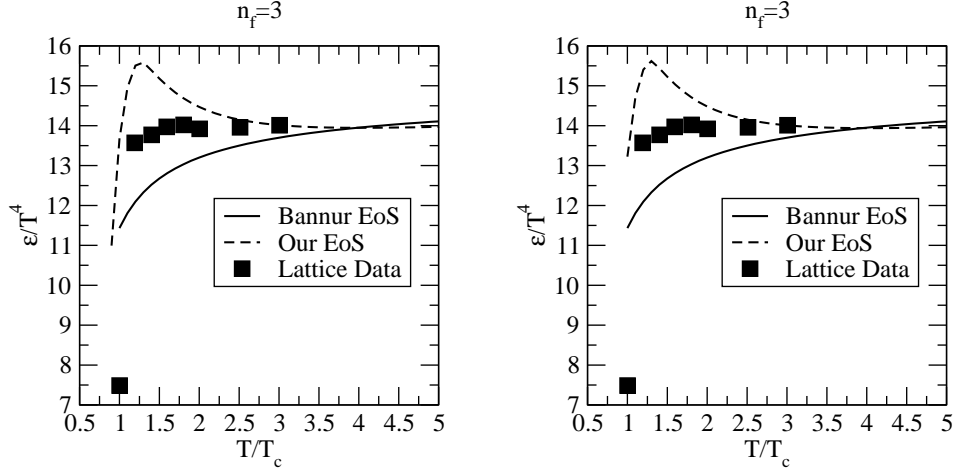


FIG. 3: Plots of ε/T^4 as a function of T/T_c for Our EoS (using quasi-particle Debye mass) and lattice results [17, 18] for 3-flavor QGP (extreme left figure) for EoS1 [11, 12], and for EoS2 [13] (extreme right figure). The notations are same as Figure2.

In our analysis, we have fixed the critical temperature ($T_c = 0.197 GeV$) and have taken the quark masses m_Q , as $m_{\Upsilon} = 4.5 GeV$, $m_{\Upsilon'} = 5.01 GeV$ and $m_{\chi_b} = 5.18 GeV$, as calculated in [22] and the string tension (σ) is taken as $0.184 GeV^2$. Let us now proceed to the computation of the dissociation temperatures for the above mentioned quarkonia bound states.

As we know, dissociation of a quarkonia bound state in a thermal QGP medium will occur whenever the binding energy, E_B of the said state will fall below the mean thermal energy of a quasi-parton. In such situations the thermal effect can dissociate the quarkonia bound state. To obtain the lower bound of the dissociation temperatures of the various quarkonia states, the (relativistic) thermal energy of the partons will $3 T$. The dissociation is supposed to occur whenever,

$$Re E_{bin}^{iso} \hat{\equiv} E_B(T_D) = 3T_D. \quad (21)$$

The T_D 's for the $b\bar{b}$ states Υ , Υ' and χ_b with the dissociation temperature are listed in Table I and II for EoS1 and EoS2 respectively. We observe that (on the basis of temperature dependence of binding energy) Υ' dissociates at lower temperatures as compared to Υ and χ_b for both the equations of state.

TABLE I: Dissociation temperature T_D (for a 3-flavor QGP), using quasi-particle debye mass for bottomonium states, for EoS1.

State	τ_F	T_D	$c_s^2(SIQGP)$	$c_s^2(Id)$	$\epsilon_s(SIQGP)$	$\epsilon_s(Id)$
Υ	0.76	1.98	0.335	1/3	24.39	23.89
Υ'	1.90	1.53	0.326	1/3	8.28	8.16
χ_b	2.60	1.61	0.331	1/3	10.21	10.10

TABLE II: Dissociation temperature T_D (for a 3-flavor QGP), using quasi-particle debye mass for bottomonium states, for EoS2.

State	τ_F	T_D	$c_s^2(SIQGP)$	$c_s^2(Id)$	$\epsilon_s(SIQGP)$	$\epsilon_s(Id)$
Υ	0.76	2.04	0.335	1/3	27.05	27.09
Υ'	1.90	1.58	0.328	1/3	9.35	9.44
χ_b	2.60	1.65	0.331	1/3	11.21	11.34

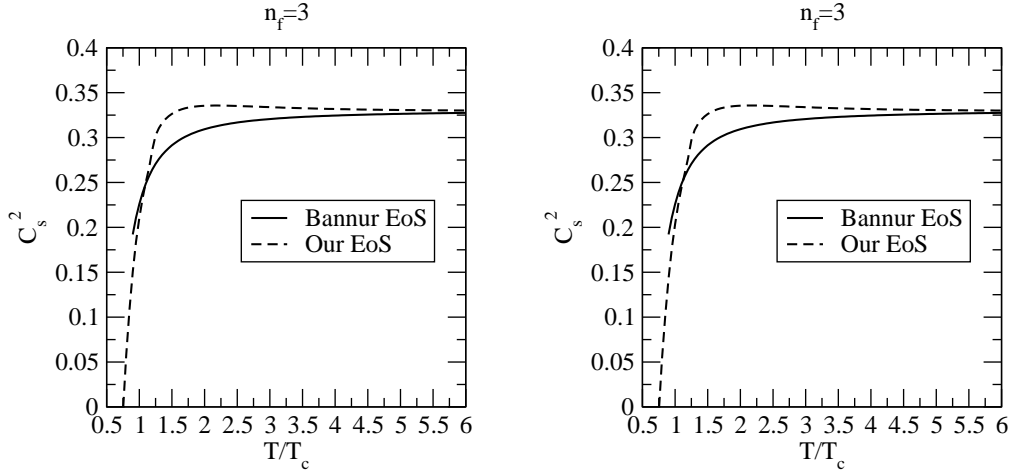


FIG. 4: Plots of c_s^2 as a function of T/T_c for Bannur EoS, Our EoS (using quasi-particle Debye mass) for 3-flavor QGP (extreme left figure) for EoS1 [11, 12], and for EOS2 [13] (extreme right figure). The notations are same as Figure2.

IV. FORMULATION

In relativistic nucleus-nucleus collisions the equation of state for the quark matter is an important observable and the properties of the matter are sensitive to it. The expansion of QGP is quite sensitive to EoS through the speed of sound, explores the sensitivity of the quarkonium suppression to the equation of state [23, 24].

For a strongly-coupled QGP Bannur [17] developed an equation of state by incorporating running coupling constant and did a appropriate modifications to take account color and flavor degrees of freedom and obtained a reasonably good fit to the lattice results. Now we will discuss briefly the equation of state which is expressed as a function of plasma parameter Γ [25]:

$$\epsilon_{\text{QED}} = \left(\frac{3}{2} + u_{ex}(\Gamma) \right) n T, \quad (22)$$

Plasma parameter Γ , is the ratio of average potential energy to average kinetic energy of particles, is assumed to be weak ($\ll 1$) and is given by:

$$\Gamma \equiv \frac{\langle PE \rangle}{\langle KE \rangle} = \frac{Re[V(\mathbf{r}, T)]}{T}, \quad (23)$$

We have studied the variation of plasma parameter with temperature and as well with the number of

flavours present in the system and are shown in Fig. 1 for EoS1 and EoS2 respectively. As the temperature increases, potential becomes weaker and hence the plasma parameter have started waning, albeit at very large temperature it increases slightly due to the contribution coming from the (positive) finite-range terms in the potential, unlike the decreasing trend in Bannur model[17] always due to the presence of Coulomb interaction alone in the deconfined phase.

Let us consider that hadron exists for $T < T_c$ and goes to QGP for $T > T_c$ for strongly-coupled plasma in QCD. As it was assumed that confinement interactions due to QCD vacuum has been melted [17] at $T = T_c$ and thus for $T > T_c$, it is the strongly interacting plasma of quarks and gluons and no glue balls or hadrons. After inclusion of relativistic and quantum effects, the equation of state which has been obtained in the plasma parameter can be written as:

$$\epsilon = \left(3 + u_{ex}(\Gamma) \right) n T, \quad (24)$$

Now, the scaled-energy density is written as in terms of ideal contribution

$$e(\Gamma) \equiv \frac{\epsilon}{\epsilon_{SB}} = 1 + \frac{1}{3} u_{ex}(\Gamma), \quad (25)$$

where ε_{SB} is given by,

$$\varepsilon_{SB} \equiv (16 + 21 n_f/2) \pi^2 T^4 / 30, \quad (26)$$

Here, n_f is the number of flavor of quarks and gluons. Now, we will employ two-loop level QCD running coupling constant in $\overline{\text{MS}}$ scheme [26],:

$$g^2(T) \approx 2b_0 \ln \frac{\bar{\mu}}{\Lambda_{\overline{\text{MS}}}} \left(1 + \frac{b_1}{2b_0^2} \frac{\ln \left(2 \ln \frac{\bar{\mu}}{\Lambda_{\overline{\text{MS}}}} \right)}{\ln \frac{\bar{\mu}}{\Lambda_{\overline{\text{MS}}}}} \right)^{-1} \quad (27)$$

Here $b_0 = (33 - 2n_f)/(48\pi^2)$ and $b_1 = (153 - 19n_f)/(384\pi^4)$. In $\overline{\text{MS}}$ scheme, $\Lambda_{\overline{\text{MS}}}$ and $\bar{\mu}$ are the renormalization scale and the scale parameter respectively. For, the EoS to depend on the renormalization scale, the physical observables should be scale independent. We invade the problem by trading off the dependence on renormalization scale ($\Lambda_{\overline{\text{MS}}}$) to a dependence on the critical temperature T_c .

$$\begin{aligned} \bar{\mu} \exp(\gamma_E + c) &= \Lambda_{\overline{\text{MS}}}(T) \\ \Lambda_{\overline{\text{MS}}}(T) \exp(\gamma_E + c) &= 4\pi\Lambda_T, \end{aligned} \quad (28)$$

here $\gamma_E = 0.5772156$ and $c = (n_c - 4n_f \ln 4) / (22n_c - n_f)$, which is a constant depending on colors and flavors. There are several incertitude, associated with the the scale parameter $\bar{\mu}$ and renormalization scale $\Lambda_{\overline{\text{MS}}}$, which occurs in the expression used for the running coupling constant α_s . This issue has been considered well in literature and resolved by the BLM criterion due to Brodsky, Lepage and Mackenzie [27]. $\Lambda_{\overline{\text{MS}}}$ is allowed to vary between πT and $4\pi T$ [29]. For our motive, we choose the $\Lambda_{\overline{\text{MS}}}$ close to the central value $2\pi T_c$ [28] for $n_f=0$ and for both $n_f=2$ and $n_f=3$ flavors the value is πT_c . If the factor

$\frac{b_1}{2b_0^2} \frac{\ln \left(2 \ln \frac{\bar{\mu}}{\Lambda_{\overline{\text{MS}}}} \right)}{\ln \frac{\bar{\mu}}{\Lambda_{\overline{\text{MS}}}}}$ is $\ll 1$ then the above expression reduces to the expression used in [17, Eq.(10)], after neglecting the higher order terms of the above factor. However, this possibility does not hold good for the temperature ranges used in the calculation and cause an error in coupling which finally makes the difference in the results between our model and Bannur model [17]. first of all, we will calculate the energy density $\varepsilon(T)$ from Eq.(25) and using the thermodynamic relation,

$$\varepsilon = T \frac{dp}{dT} - P, \quad (29)$$

we calculated the pressure as

$$\frac{P}{T^4} = \left(\frac{P_0}{T_0^4} + 3a_f \int_{T_0}^T d\tau \tau^2 e(\Gamma(\tau)) \right) / T^3, \quad (30)$$

here P_0 is the pressure at some reference temperature T_0 . Now, the speed of sound $c_s^2 (= \frac{dP}{d\varepsilon})$ can be calculated once we know the pressure P and energy density ε .

V. SURVIVAL OF BOTTOMONIUM STATE

In order to derive the Υ survival probability for an expanding QGP firstly, we explore the effects of dissipative terms up to first-order in the stress-tensor. In the presence of viscous forces, the energy-momentum tensor is written as,

$$T^{\mu\nu} - \pi^{\mu\nu} = (\epsilon + p)u^\mu u^\nu + g^{\mu\nu}p, \quad (31)$$

where the stress-energy tensor, $\pi^{\mu\nu}$ up to first-order is given by

$$\pi^{\mu\nu} = \eta \langle \nabla^\mu u^\nu \rangle, \quad (32)$$

where η is the co-efficient of the shear viscosity and $\langle \nabla^\mu u^\nu \rangle$ is the symmetrized velocity gradient.

In Bjorken expansion, the equation of motion is given by

$$\partial_\tau \epsilon + \frac{\epsilon + p}{\tau} = \frac{4\eta}{3\tau^2}. \quad (33)$$

The solution of equation of motion (33) is given as,

$$\begin{aligned} \epsilon(\tau) \tau^{(1+c_s^2)} + \frac{4a}{3\tilde{\tau}^2} \tau^{(1+c_s^2)} &= \epsilon(\tau_i) \tau_i^{(1+c_s^2)} + \frac{4a}{3\tilde{\tau}_i^2} \\ &= \text{const}, \end{aligned} \quad (34)$$

where the constant

$$a = \left(\frac{\eta}{s} \right) T_i^3 \tau_i \quad (35)$$

and the symbols,

$$\tilde{\tau}^2 = (1 - c_s^2) \tau^2 \quad (36)$$

and

$$\tilde{\tau}_i^2 = (1 - c_s^2) \tau_i^2. \quad (37)$$

The first term accounts for the contributions coming from the zeroth-order expansion (ideal fluid) and the second term is the first-order viscous corrections. We now have all the ingredients to write down the survival probability. Chu and Matsui [33] studied the transverse momentum dependence (p_T) of the survival probability by choosing the speed of sound $c_s^2 = 1/3$ (ideal EoS) and the extreme value $c_s^2 = 0$. Instead of taking arbitrary values of c_s^2 we tabulated the values of c_s^2 in Tables I and II corresponding to the dissociation temperatures for bottomonium

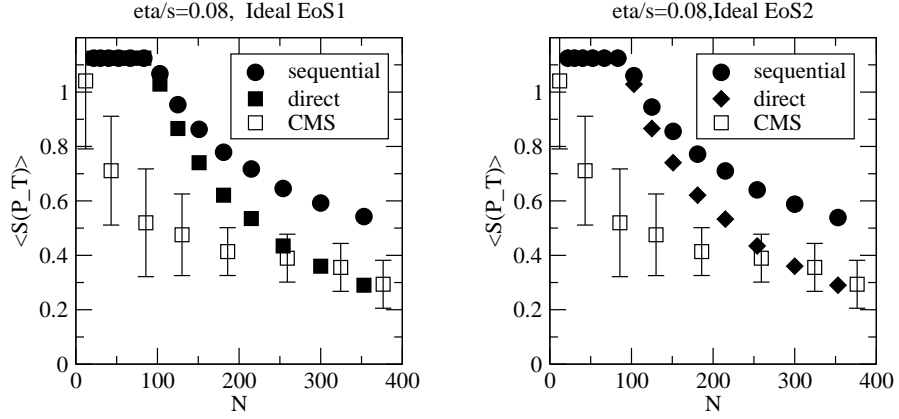


FIG. 5: The variation of p_T integrated survival probability versus N for Υ at $\sqrt{S_{NN}} = 2.76$ TeV with preliminary CMS data [30]. The experimental data are shown by the squares with error bars whereas circles and diamond represent with $\langle S^{\text{incl}} \rangle$ without $\langle S^{\text{dir}} \rangle$ sequential melting using the value of T_D 's and related parameters from Table I and Table II for Ideal equation of state. Left panel shows EoS1 and right panel shows EoS2 .

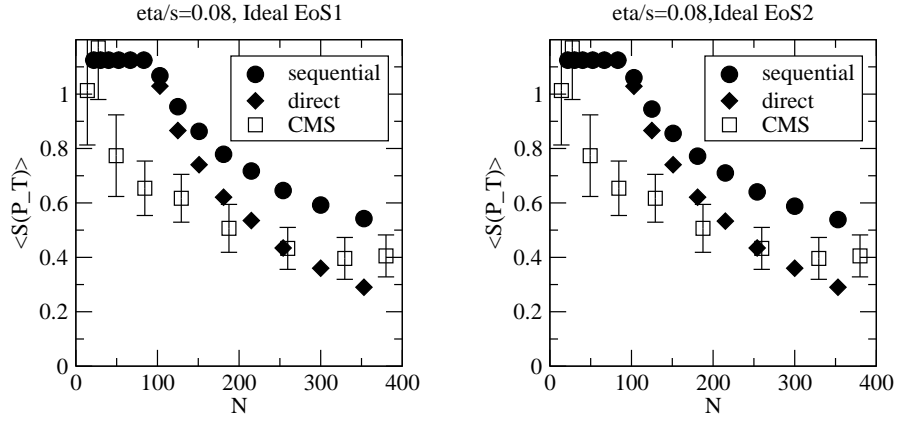


FIG. 6: Same as Fig.5 but the variation of p_T integrated survival probability versus N for Υ at $\sqrt{S_{NN}} = 5.02$ TeV with preliminary CMS data [31].

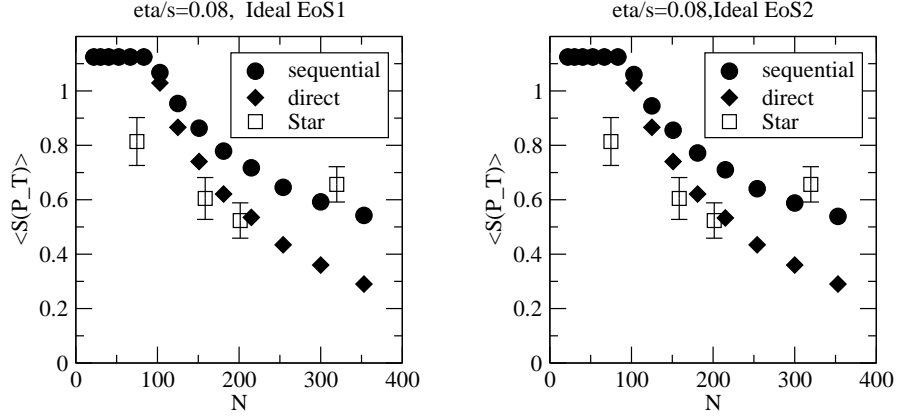


FIG. 7: Same as Fig.5 but the variation of p_T integrated survival probability versus N for Υ at $\sqrt{s_{NN}} = 200$ GeV with preliminary STAR data [32].

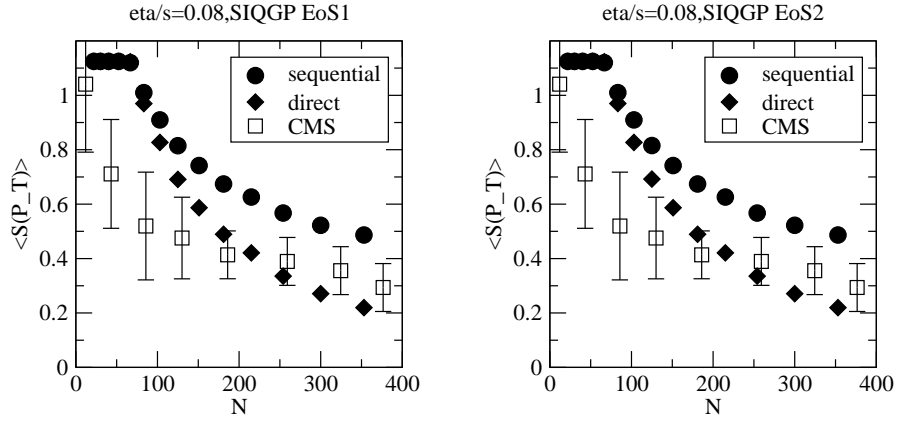


FIG. 8: The variation of p_T integrated survival probability versus N for Υ at $\sqrt{s_{NN}} = 2.76$ TeV with preliminary CMS data [30]. The experimental data are shown by the squares with error bars whereas circles and diamond represent with $\langle S^{\text{incl}} \rangle$ without $\langle S^{\text{dir}} \rangle$ sequential melting using the value of T_D 's and related parameters from Table I and Table II for SIQGP equation of state. Left panel shows EoS1 and right panel shows EoS2.

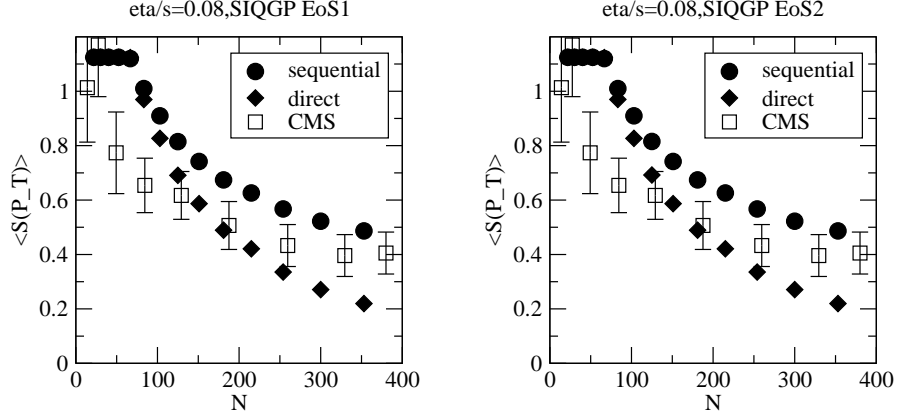


FIG. 9: Same as Fig.8 but the variation of p_T integrated survival probability versus N for Υ at $\sqrt{S_{NN}} = 5.02$ TeV with preliminary CMS data [31].

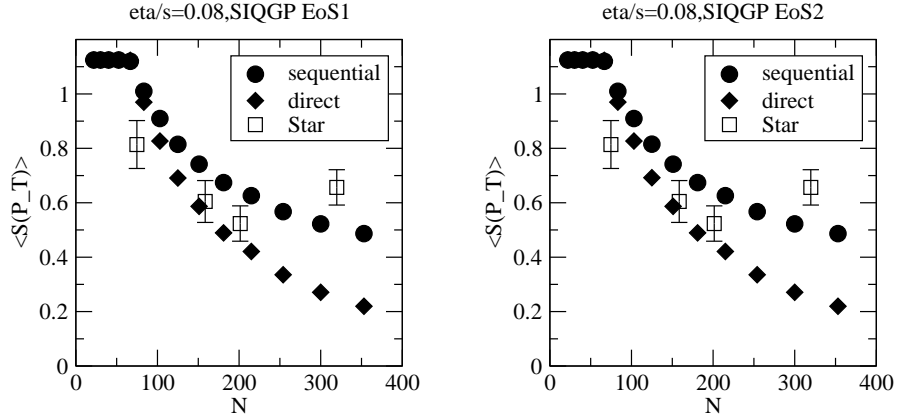


FIG. 10: Same as Fig.8 but the variation of p_T integrated survival probability versus N for Υ at $\sqrt{S_{NN}} = 200$ GeV with preliminary STAR data [32].

states for EOS1 and EOS2. One can define initial energy density ϵ_i as

$$\epsilon_i = (1 + \beta)\langle\epsilon_i\rangle \quad ; \beta = 1. \quad (38)$$

Here, β represents the proportionality of the deposited energy to the nuclear thickness whereas $\langle\epsilon_i\rangle$ is the average initial energy density and will be given by the modified Bjorken formula [34, 35]:

$$\langle\epsilon_i\rangle = \frac{\xi}{A_T \tau_i} \left(\frac{dE_T}{dy_h} \right)_{y_h=0}, \quad (39)$$

where A_T is the transverse overlap area of the colliding nuclei and $(dE_T/dy_h)_{y_h=0}$ is the transverse energy deposited per unit rapidity. we use the experimental value of the transverse overlap area A_T and the pseudo-rapidity distribution $dE_T/d\eta_h|_{\eta_h=0}$ [36] at various values of number of participants N_{part} . These $dE_T/d\eta_h|_{\eta_h=0}$ numbers are then multiplied by a Jacobian 1.25 to yield the rapidity distribution $dE_T/dy_h|_{y_h=0}$ which will be further used to calculate the average initial energy density from Bjorken formula (39). After getting the value of average initial energy density we can obtain the initial energy density from the formula (38). The scaling factor $\xi = 5$ has been introduced in order to obtain the desired values of initial energy densities [37] for most central collision which are consistent with the predictions of the self-screened parton cascade model [38] and also with the requirements of hydrodynamic simulation [37] to fit the pseudo-rapidity distribution of charged particle multiplicity $dN_{ch}/d\eta$ for various centralities observed in PHENIX experiments at RHIC energy. Let ϕ is the angle between the transverse momentum and position vector r_Υ . Now assuming that $b\bar{b}$ is formed inside screening region at a point whose position vector is \vec{r} and moves with transverse momentum p_T making an azimuthal angle. Then the condition for escape of $b\bar{b}$ without forming bottomonium states is expressed as:

$$\cos\phi \geq Y; \quad Y = \frac{(r_s^2 - r_\Upsilon^2)m - \tau_F^2 p_T^2/m}{2r_\Upsilon \tau_F p_T}, \quad (40)$$

where, r_Υ is the position vector at which the bottom, anti bottom quark pair is formed, τ_F is the proper formation time required for the formation of bound states of $b\bar{b}$ from correlated $b\bar{b}$ pair and m is the mass of bottomonia ($m = M_\Upsilon, M_{\chi_b}, M_{\Upsilon'}$ for different resonance states of bottomonium). Assuming the radial probability distribution for the production of $b\bar{b}$ pair in hard collisions at transverse distance r as

$$f(r) \propto \left(1 - \frac{r^2}{R_T^2}\right)^\alpha \theta(R_T - r). \quad (41)$$

Here we take $\alpha = 0.5$ in our calculation as used in Ref. [33]. Then, in the colour screening scenario, the

survival probability for the bottomonium in QGP medium can be expressed as [33, 39] :

$$S(p_T, N_{part}) = \frac{2(\alpha + 1)}{\pi R_T^2} \int_0^{R_T} dr r \phi_{max}(r) \left\{ 1 - \frac{r^2}{R_T^2} \right\}^\alpha, \quad (42)$$

where the maximum positive angle ϕ_{max} allowed by Equation 26 becomes [40] :

$$\phi_{max}(r) = \begin{cases} \pi & \text{if } Y \leq -1 \\ \pi - \cos^{-1}|Y| & \text{if } 0 \geq Y \geq -1 \\ \cos^{-1}|Y| & \text{if } 0 \leq Y \leq 1 \\ 0 & \text{if } Y \geq 1 \end{cases}$$

since the experimentalists always measure the quantity namely p_T integrated nuclear modification factor. We get the theoretical p_T integrated survival probability as follows :

$$S(N_{part}) = \frac{\int_{p_{Tmin}}^{p_{Tmax}} S(p_T, N_{part}) dp_T}{\int_{p_{Tmin}}^{p_{Tmax}} dp_T}. \quad (43)$$

In nucleus-nucleus collisions, it is known that only about 60% of the observed Υ originate directly in hard collisions while 30% of them come from the decay of χ_b and 10% from the decay of Υ' . Hence, the p_T -integrated inclusive survival probability of Υ in the QGP becomes [23, 41].

$$\langle S^{incl} \rangle = 0.6 \langle S^{dir} \rangle_\Upsilon + 0.3 \langle S^{dir} \rangle_{\chi_b} + 0.1 \langle S^{dir} \rangle_{\Upsilon'} \quad (44)$$

VI. RESULTS AND DISCUSSIONS

In our results we had obtained the variation of plasma parameter with temperature and as well with the number of flavours present in the system and are shown in Fig. 1 for EoS1 and EoS2 respectively. After then, in Fig. 2, we have plotted the variation of pressure (P/T^4) with temperature (T/T_c) using EoS1 and EoS2 for 3-flavor QGP along with Bannur EoS [17] and compared it with lattice results [17, 18]. For each flavor, g_c and Λ_T are adjusted to get a good fit to lattice results in Bannur Model. Now, energy density ϵ , speed of sound c_s^2 etc. can be derived since we had obtained the pressure, $P(T)$. In Fig. 3, we had plotted the energy density (ϵ/T^4) with temperature (T/T_c) using EoS1 [11, 12] and EoS2 for 3-flavor QGP along with Bannur EoS [17] and compared it with lattice result [17, 18]. As the flavor increases, the curves shifts to left. In Fig. 4, the speed of sound, c_s^2 is plotted for all three systems, using EoS1 and EoS2 for 3-flavor QGP along with Bannur EoS [17]. Since lattice results are not available for 3-flavor, therefore comparison has not

been checked for the above mentioned flavor. Our flavored results matches excellent with the lattice results. We observe that as the flavor increases c_s^2 becomes larger for both EoS1 and EoS2. All three curves shows similar behaviour, i.e, sharp rise near T_c and then flatten to the ideal value (1/3).

In this paper we had calculated the dissociation temperatures for the bottomonium states (Υ , Υ' , χ_b , etc.), by modifying the Cornell potential and incorporating the quasi-particle debye mass. On that dissociation temperature we had calculated the screening energy densities, ϵ_s and the speed of sound c_s^2 which are also listed in the table I and II for both EoS1 and EoS2 respectively. We observe from the table I- II that the value of ϵ_s is different for different bottomonium states and varies from one EoS to other. If $\epsilon_s \gtrsim \epsilon_i$, initial energy density, then there will be no suppression at all i.e., survival probability, $S(p_T)$ is equal to 1. With this physical understanding we analyze our results, $\langle S(p_T) \rangle$ as a function of the number of participants N_{part} in an expanding QGP.

Here we are using the values as inputs listed in Table I and Table II, to calculate $\langle S(p_T) \rangle$ for both EOS1 and EOS2 respectively. The experimental data (the nuclear-modification factor R_{AA}) are shown by the squares with error bars whereas circles represent sequential suppression. We had compared our results with the experimental results for the case of $\eta/s = 0.08$ for both EoS1 and EoS2 and found good agreement. We observe from the figs. 5-10 that $\langle S(p_T) \rangle$ for both the directly and sequentially produced Upsilon (Υ) are quite high with the higher values of T_D 's which is obtained from EOS2 (in Table II) compared to EOS1 (in Table I) for both SIQGP and Ideal equation of states. We find that the survival probability of sequentially produced Υ is slightly higher compared to the directly produced Υ and is closer to the experimental results. We also observed that sequentially produced Υ nicely matches for the EOS1 compared to the EOS2. The smaller value of screening energy density ϵ_s causes an increase in the screening time and results in more suppression to match with the experimental results.

VII. CONCLUSIONS

We studied the equation of state for strongly interacting quark-gluon plasma in the framework of

strongly coupled plasma with appropriate modifications to take account of color and flavor degrees of freedom and QCD running coupling constant. In addition, we incorporate the nonperturbative effects in terms of nonzero string tension in the deconfined phase, unlike the Coulomb interactions alone in the deconfined phase beyond the critical temperature. Our results on thermodynamic observables *viz.* pressure, energy density, speed of sound etc. nicely fit the results of lattice equation of state. We had then calculated the dissociation temperatures for the bottomonium states (Υ , Υ' , χ_b , etc.), by incorporating the quasi-particle debye mass. On that dissociation temperature we had calculated the screening energy densities, ϵ_s and the speed of sound c_s^2 which are listed in the table I and II for both EoS1 and EoS2 respectively. By using the above quantities as a input we have then studied the sequential suppression for bottomonium states at the LHC energy in a longitudinally expanding partonic system, which underwent through the successive pre-equilibrium and equilibrium phases in the presence of dissipative forces. Bottomonium suppression in nucleus-nucleus collisions compared to p - p collisions couples the in-medium properties of the bottomonia states with the dynamics of the expanding medium. We have found a good agreement with the experimental data from RHIC 200GeV/nucleon Au-Au collisions, LHC 2.76 TeV/nucleon Pb-Pb, and LHC 5.02 TeV/nucleon Pb-Pb collisions [42, 43]. Here our attempt is to understand Υ suppression systematically in SIQGP in anisotropic medium. It would be of interest to extend the present study by incorporating the contributions of the bulk viscosity. These issues will be taken up separately in the near future.

VIII. ACKNOWLEDGEMENT

VKA acknowledge the UGC-BSR research start up grant No. F.30-14/2014 (BSR) New Delhi. We record our sincere gratitude to the people of India for their generous support for the research in basic sciences.

-
- [1] T. Matsui and H. Satz, Phys. Lett. B **178**, 416 (1986).
 - [2] F. Karsch, M. T. Mehr, H. Satz, Z. Phys. C **37**, 617 (1988); F. Karsch, H. Satz, Z. Phys. C **51**, 209 (1991).
 - [3] STAR Collaboration (John Adams *et al.*),

- Nucl.Phys. **A757**, 102 (2005); PHENIX Collaboration (K. Adcox *et al.*), Nucl.Phys. **A757**, 184, (2005); B.B. Back et al., Nucl.Phys. **A757**, 28 (2005).
- [4] H. J. Drescher, A. Dumitru, C. Gombeaud, J. Y. Ollitrault, Phys. Rev. C **76**, 024905 (2007).

- [5] E. Shuryak, Nucl.Phys. **A774**, 387 (2006).
- [6] P.Kovtun, D.T.Son, A.O.Starinets, Phys. Rev. Lett. **94**, 111601 (2005).
- [7] Vinod Chandra, A. Ranjan, V. Ravishankar, Euro. Phys. J C **40**, 109 (2009).
- [8] Vinod Chandra, R. Kumar, V. Ravishankar, Phys.Rev.C **76**, 054909 (2007).
- [9] Vinod Chandra and V.Ravishankar, Eur.Phys.J.C **64**, 63-72 (2009).
- [10] V. Agotiya, V. Chandra and B. K. Patra, Phys. Rev. C **80**, 025210 (2009).
- [11] C. Zhai and B. Kastening, Phys. Rev. **52**, 7232 (1995).
- [12] P. Arnold and C. Zhai, Phys. Rev. D**50**, 7603 (1994); Phys. Rev.D **51**, 1906 (1995).
- [13] K. Kajantie, M. Laine, K. Rummukainen, Y. Schroder Phys. Rev. D **67**, 105008 (2003).
- [14] A. Schneider Phys. Rev. D **66**, 036003 (2002).
- [15] H. A. Weldon, Phys. Rev. D **26**, 1394 (1982).
- [16] J. I. Kapusta and C. Gale, *Finite Temperature Field Theory Principle and Applications* (Cambridge University Press, Cambridge, 1996), 2nd ed.
- [17] V. M. Bannur, J. Phys. G: Nucl. Part. Phys. **32** (2006) 993.
- [18] G.boyd et al.,Phys.Rev.Lett. **75** (1995) 4169 ; Nucl.Phys.B **469** (1996) 419 ;F. Karsch, Lect. Notes Phys. **583** (2002) 209; A. Bavavov et, arXiv:0903.4379.
- [19] Y. Burnier, M. Laine, M. Vepsäläinen, Phys. Lett. B **678**, 86 (2009).
- [20] V.K.Agotiya, V.Chandra, M.Y. Jamal , I. Nilima, Phys. Rev. D **94**, 094006 (2016).
- [21] Lata Thakur, Uttam Kakade and Binoy Krishna Patra, Phys. Rev.D **89**(2014) 094020.
- [22] V. M. Aulchenko *et al.* [KEDR Collaboration], Phys. Lett. B **573**, 63 (2003).
- [23] D. Pal, B. K. Patra and D. K. Srivastava, Euro. Phys. J. **C 17**, 179 (2000).
- [24] B. K. Patra and D. K. Srivastava, Phys. Lett. B **505** (2001) 113 .
- [25] S. Ichimaru, *Statistical Plasma Physics (Vol. II) -Condensed Plasma* (Addison-Wesley Publishing Company, 1994 New York,).
- [26] M. Laine, Y. Schroder, JHEP **0503** (2005) 067 .
- [27] Suzhou Huang, Marcello Lissia, Nucl.Phys.B **438** (1995) 54.
- [28] A. Vuorinen, arXiv:hep-ph/0402242.
- [29] E. Braaten and A. Neito, Phys. Rev. D **53** (1996) 3421 (hep-ph/9510408).
- [30] CMS Collaboration Twiki, CMS-PAS-HIN-10-006,2015.
- [31] Chad Flores (ALICE Collaboration), Quark matter 2017, <https://goo.gl/imTtmM>, 2017.
- [32] Zaochen Ye (STAR Collaboration), Quark matter 2017, <https://goo.gl/XgqSgG>, 2017.
- [33] M. C. Chu and T. Matsui, Phys. Rev. D **37**, 1851 (1988).
- [34] NA50 collaboration, B. Alessandro et al., Eur. Phys. J. C **39** (2005) 335 [hep-ex/0412036].
- [35] F. Karsch, D. Kharzeev and H. Satz, Phys. Lett. B **637**, 75 (2006).
- [36] S. S. Adler et al., (PHENIX Collaboration), Phys. Rev. C **71**, 034908 (2005); S. S. Adler et al., (PHENIX Collaboration), Phys. Rev. C **71**, 049901(E) (2005).
- [37] T. Hirano, Phys. Rev. C **65**, 011901(R) (2001); T. Hirano and K. Tsuda, Phys. Rev. C **66**, 054905 (2002).
- [38] K. J. Eskola, K. Kajantie, P. V. Ruuskanen, and K. Tuominen, Nucl. Phys. **B570**, 379 (2000).
- [39] M. Mishra, C. P. Singh, V. J. Menon and Ritesh Kumar Dubey, Phys. Lett. **B 656**, 45 (2007); M. Mishra, C. P. Singh and V. J. Menon, Proc. of QM, Indian. J. Physics **85**, 849 (2011).
- [40] Vineet Agotiya, Lata Devi, Uttam Kakade, Binoy Krishna Patra International Journal of Modern Physics A **27**,02,(2012).
- [41] H. Satz, Nucl. Phys. **A783**, 249 (2007). [arXiv:hep-ph/0609197].
- [42] Brandon Krouppa, Radoslaw Ryblewski,Michael Strickland, Nuclear Physics A **00**, 1-4 (2017).
- [43] Brandon Krouppa, R. Ryblewski,Michael Strickland, Phys. Rev. C **92**, 061901 (2015).